JOURNAL OF QUATERNARY SCIENCE (2020) 1–12 ISSN 0267-8179. DOI: 10.1002/jqs.3196

JQS Journal of Quaternary Science QRA Quaternary Research Association

# Reconstruction of the Late Holocene climate and environmental history from North Bolgoda Lake, Sri Lanka, using lipid biomarkers and pollen records

KASUN GAYANTHA,[1] JOYANTO ROUTH,[2]* KRISHNAMURTHY ANUPAMA,[3] JEAN LAZAR,[3] SRINIVASAN PRASAD,[3] ROHANA CHANDRAJITH,[4] PATRICK ROBERTS[5] and GERD GLEIXNER[1]

[1]Max Planck Institute for Biogeochemistry, Jena, Germany
[2]Department of Thematic Studies – Environmental Change, Linköping University, Linköping, Sweden
[3]Laboratory of Palynology & Paleoecology, Department of Ecology, French Institute of Pondicherry, Pondicherry, India
[4]Department of Geology, Faculty of Science, University of Peradeniya, Peradeniya, Sri Lanka
[5]Max Planck Institute for the Science of Human History, Jena, Germany

Received 18 September 2019; Revised 25 December 2019; Accepted 1 March 2020

ABSTRACT: The catastrophic impact and unpredictability of the Indian Ocean Monsoon (IOM) over South Asia are evident from devastating floods, mudslides and droughts in one of the most densely populated regions of the globe. However, our understanding as to how the IOM has varied in the past, as well as its impact on local environments, remains limited. This is particularly the case for Sri Lanka, where erosional landscapes have limited the availability of well-stratified, high-resolution terrestrial archives. Here, we present novel data from an undisturbed sediment core retrieved from the coastal Bolgoda Lake. This includes the presentation of a revised Late Holocene age model as well as an innovative combination of pollen, source-specific biomarkers, and compound-specific stable carbon isotopes of *n*-alkanes to reconstruct the shifts in precipitation, salinity and vegetation cover. Our record documents variable climate between 3000 years and the present, with arid conditions c. 2334 and 2067 cal a BP. This extreme dry period was preceded and followed by more wet conditions. The high-resolution palaeoenvironmental reconstruction fills a major gap in our knowledge on the ramifications of IOM shifts across South Asia and provides insights during a time of major redistribution of dense human settlements across Sri Lanka. © 2020 The Authors Journal of Quaternary Science Published by John Wiley & Sons Ltd.

KEYWORDS: biomarker; carbon isotopes; monsoon; palaeosalinity; pollen.

## Introduction

Seasonal migration of the Inter-Tropical Convergence Zone (ITCZ) over the equatorial region drives the Indian Ocean Monsoon (IOM) system that brings water for agriculture and drinking purposes to one of the most densely populated parts of the globe. The IOM dictates the amount of precipitation and distribution of vegetation across the vastly diverse landmass of South Asia (Tierney et al., 2008), with the region being extremely sensitive to annual fluctuations in its position and intensity. Variability in the IOM has led to the increasing frequency of extreme events, such as flash floods, mudslides, or droughts (Ratnayake and Herath, 2005; Mirza, 2011). This is particularly the case for the island of Sri Lanka, which sits at an equatorial position in the Indian Ocean and has experienced an increasing frequency of extreme events that have serious consequences for human mortality, disruption and loss of property (Zubair et al., 2006). Changes in the ITCZ and IOM in the past would almost certainly have had similar dramatic consequences for South Asian environments and dense human populations in the recent past, with potential insights into the likely tempo and nature of future changes. Yet high-resolution, multi-disciplinary palaeoenvironmental records remain conspicuously rare for many parts of South Asia.

Sri Lanka is an ideal place to reconstruct past changes in the ITCZ and IOM, given its central position in the Indian Ocean and the sensitivity of terrestrial landscapes to fluctuations in precipitation. The central highlands of Sri Lanka, with a maximum altitude of 2524 m a.s.l., act as an orographic barrier, confining the moisture-rich summer (southwest) monsoon to the southwestern part of the island. Meanwhile, the retreating winter (northeast) monsoon affects the northeastern part of the island. These monsoons result in the development of local climate zones that are identified as wet, dry and intermediate (Malmgren et al., 2003; Fig. 1). Significant sub-millennial IOM variability has been highlighted for Late Holocene South Asia (Moy et al., 2002; Ponton et al., 2012), and may have led to increasing aridity and unpredictability of rainfall in southern India (Fuller et al., 2007; Roberts et al., 2015), as well as the northern dry zone in Sri Lanka (Gilliland et al., 2013). While some palaeoenvironmental records exist for Sri Lanka, tracing the changes in monsoon intensity (Premathilake and Risberg, 2003; Premathilake and Gunatilaka, 2013; Gayantha et al., 2017; Ratnayake et al., 2017), they are poorly dated, analysed using a few palaeoenvironmental proxies, or represent environmentally and spatially isolated sites far from key centres of past and present human agriculture or urban centres. The paucity of sedimentary archives is, in part, a consequence of the fact that intense erosional surfaces are a product of the steep geomorphological setting in Sri Lanka, which limits the formation of sedimentary repositories such as natural lakes.

Bolgoda Lake, a semi-closed, brackish archive, with limited marine influence, is emerging as a promising locale for studying terrestrial Holocene palaeoenvironmental changes

*Correspondence: Joyanto Routh, as above.
E-mail: joyanto.routh@liu.se

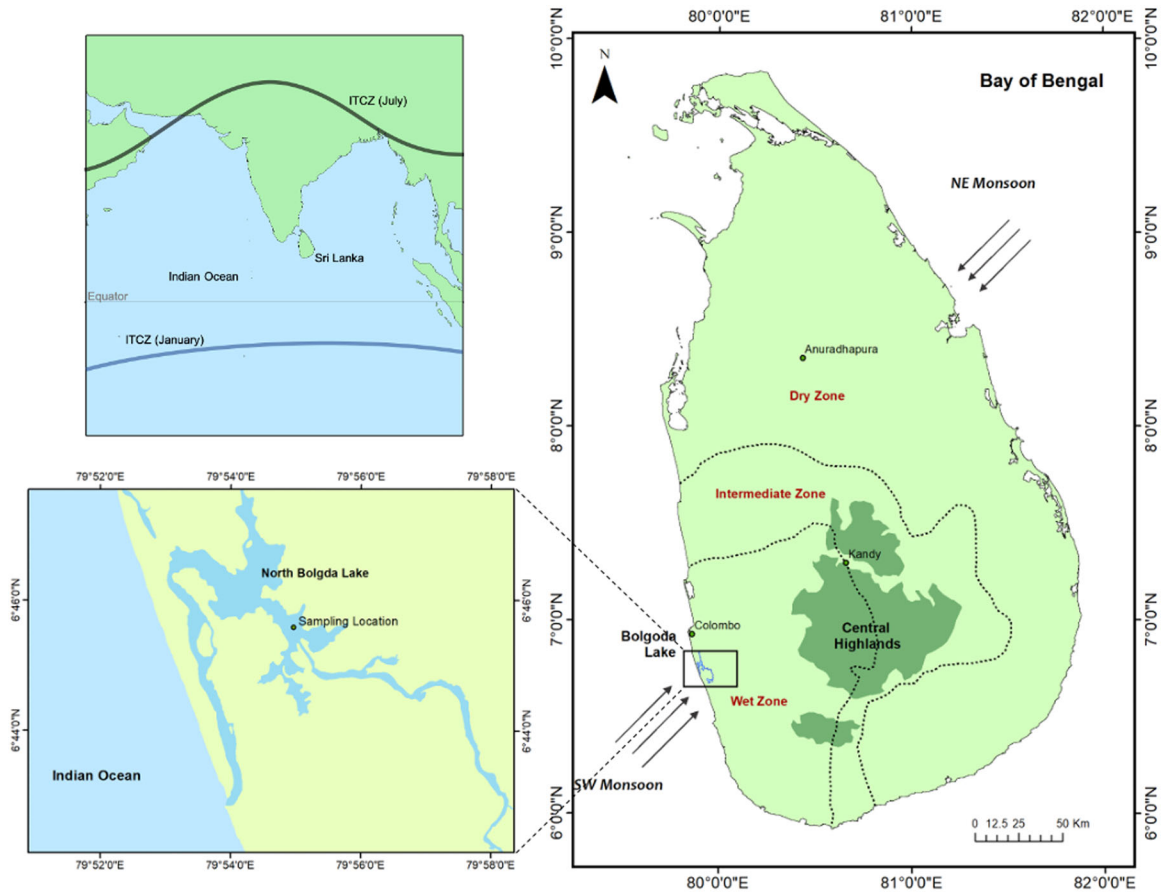


**Figure 1.** The geographical location of Sri Lanka in the path of the Inter-Tropical Convergence Zone (ITCZ) (top left), southwest and northeast monsoon pathways and climate zones in Sri Lanka (right) and sampling location in the Bolgoda Lake (bottom left). [Color figure can be viewed at wileyonlinelibrary.com]

in southwestern Sri Lanka (Gayantha et al., 2017; Ratnayake et al., 2017, 2019). However, uncertainties of dating and a lack of the application of molecular level palaeoenvironmental proxies, which have been shown to provide a greater environmental resolution than bulk or traditional approaches, necessitate further study. Tropical coastal water bodies like Bolgoda Lake are normally surrounded by thriving mangrove vegetation that has become one of the major organic matter (OM) sources of the lake or lagoon sediments. The trees possess special adaptations for surviving under different saline and arid conditions that control the density and species proportion under mangrove cover (Kumaran et al., 2005; Goldstein and Santiago, 2016). Therefore, quantitative analysis of geochemical signatures specific to the mangrove vegetation, together with pollen counts, can provide important information about the fluctuations in salinity, arid conditions and related environmental settings.

We focus on a 4.1 m long sediment core in order to reconstruct the Late Holocene climate and environmental history of western Sri Lanka. We apply radiocarbon dating to mollusc shells in order to constrain the age of the core, while combining source-specific diagnostic biomarkers (*n*-alkanes, *n*-alkanoic acids, *n*-alkanols and triterpenols), compound-specific carbon isotope signature in *n*-alkanes and traditional pollen analysis. This record gives us the opportunity to develop the most comprehensive understanding of fluctuations in vegetation and landscape changes in the vicinity of the capital of Colombo to date. Furthermore, given that significant and unequivocal variability in IOM impact on environments located away from the core monsoon region has been demonstrated (Premathilake and Risberg, 2003; Prasad et al., 2014; Mishra et al., 2019), this dataset enables us to develop a more spatially nuanced understanding of IOM impacts in South Asia.

## Background, materials and methods

### *Study area and site*

The climate of Sri Lanka can be divided into four seasons. This includes two principal monsoon seasons that are the southwest monsoon which occurs from May to September (annual rainfall >2500 mm) and the northeast monsoon that occurs from December to February (annual rainfall <1750 mm). In addition, two inter-monsoon seasons occur as a result of convections occurring from March to April and October to November (Malmgren et al., 2003). The mean annual temperature is around 27 °C and the annual rainfall is ~2500 mm (Ranwella, 1995; Malmgren et al., 2003). The annual rainfall on the island not only defines the boundaries of its primary climate zones (i.e. wet, dry and intermediate) but also its vegetation.

The Bolgoda Lake system is a semi-closed brackish water body (Ratnayake et al., 2017) located on the west coast of Sri Lanka (6°40′56″–6°48′47″ N, 79°53′55″–79°58′25″ E; Fig. 1). This lake drains a substantial area of 374 km$^2$ wedged between the western parts of the Kalu and Kelani River basins (Ranwella, 1995). The lake consists of two interconnected basins – the North Bolgoda Lake and South Bolgoda Lake. North Bolgoda Lake is shallow and the average depth is ca. 2–3 m (Gayantha et al., 2017). It is connected to the Indian Ocean through a narrow estuary and the lake basin is located c. 2 m a.m.s.l. The impact of wave action and currents is negligible in the lake. However, limited seawater intrusion is possible as a result of low lake levels during the dry season and limited discharge into the lake (Ratnayake et al., 2018). The catchment and the basement beneath the lake consist of low permeability high-grade metamorphic rocks charnockitic

 

gneiss, biotite gneiss and undifferentiated Proterozoic gneiss (GSMB, 1996).

The wet zone, where the Bolgoda Lake lies, is characterised by rainforests and grasslands, whereas the dry zone is characterised by semi-evergreen forests, grasslands and shrubs, and monsoon scrub jungles (Erdelen, 1988). Aquatic vegetation in the lake consists of *Potamogeton indicus*, *Aponogeton*, *Limnophila* and *Nymphaea*, whereas *Utricularia*, *Bacopa*, *Monochorai* and *Ceratopteris* dominate the surrounding marshy areas. These wetlands are flanked by bushy woodlands consisting mainly of *Anona*, *Melastoma*, *Memecylon*, *Wormia*, *Osbeckia* and *Syzygium*. Large trees are sparse and *Sonneratia*, *Dillenia* and *Cerbera* are common. *Nipa* is the only naturally occurring palm that covers a significant area along the lake border (Ranwella, 1995). Mangrove vegetation, including *Avicennia*, *Rhizophora*, *Bruguiera* and *Sonneratia*, is common around the lake (Jayatissa et al., 2002). The lake is bordered by small residential settlements that depend on agriculture. Rice is the major food crop grown in the region and paddy fields cover large parts of the catchment.

## Sampling

The sampling location (06°45′32″ N, 79°55′09″ E) was selected as the deepest point of North Bolgoda Lake and marks the entry point of an inland stream into the northern edge of the lake (Fig. 1). This location was selected after an initial survey of the lake with a view to minimising the direct influence of the Indian Ocean. A mechanical piston corer was used to retrieve an undisturbed 4.1 m long sediment core. Lithological characteristics (colour, grain size and sediment texture) were recorded visually along with information on the presence of carbonaceous shells, wood and charcoal (Gayantha et al., 2017). The whole sediment core was sliced into 0.5 cm sections and freeze dried before being processed for the diagnostic biomarkers and pollen.

## Age–depth model

We present a revised age model compared with Gayantha et al. (2017), with a new mollusc shell $^{14}C$ age at 25 cm depth ($F^{14}C = 0.8442 \pm 0.0041$), analysed at the Max Planck Institute for Biogeochemistry, Jena, Germany. Due to the close proximity to the Indian Ocean, all the $^{14}C$ dates in mollusc shells were calibrated using the Marine13 curve (Reimer et al., 2013) and corrected for the local marine reservoir age ($\Delta R = 133 \pm 65$) based on data from the online Marine Reservoir Database at Queen's University, Belfast, UK. The age–depth model for the sediment core was developed based on the R software package BACON (Blaauw and Christen, 2011) which uses Bayesian statistics. In this revised model (Fig. 2), a boundary was marked at 60 cm depth that indicates a significantly lower accumulation rate to the top of the core. The boundary is not a hiatus but represents a transition to an upper clayey interval with low sedimentation. The mean accumulation rate for the section between 395 and 60 cm was 5 a/cm, whereas the section between 60 and 0 cm was 22 a/cm.

## Biomarker analysis

Some 3–7 g of 40 freeze-dried sediment samples were used to extract the lipid fraction using dichloromethane and methanol mixture (9:1 v/v) on a Dionex ASE 300 Accelerated Solvent Extractor. The total lipid extract (TLE) was then concentrated on a Büchi Syncore. The extract was dried under nitrogen and weighed and re-dissolved in 300 µl of dichloromethane (DCM): isopropanol (IPA) mixture (2:1 v/v). The solid phase extraction (SPE) technique was applied (see Ghosh et al., 2015) with minor modifications to the original method proposed by Wakeham et al. (2002) to separate the neutral and acid fractions from TLEs using the aminopropyl LC-$NH_2$ cartridges (Supelco). The neutral fraction was eluted with the DCM:IPA mixture (2:1 v/v) and the solvent volume was reduced. The SPE cartridge was further eluted for the acid fraction (fatty acids) using 2% acetic acid in diethyl ether and the extract volume was reduced. The acid fraction was derivatised with 14% $BF_3$ in methanol at 100 °C for 2 h. The neutral fraction was further separated into alkanes (non-polar fraction) with 5 ml of hexane. Alcohol and sterol (polar fraction) were eluted with 5 ml of DCM:methanol (2:1 v/v) mixture using the Bond Elut Alumina-N cartridges (Supelco). After that, the extract volume was reduced by evaporation on a Büchi Syncore and reduced to dryness under nitrogen. The alkane fraction was re-dissolved in 1 ml of hexane and then an aliquot of 180 µl of the sample was spiked with 20 µl of internal standard (deuterated-tetracosane and androstane mixture) for quantification. The polar fraction (alcohol and sterol) was derivatised with bis(trimethylsilyl)trifluoroacetamide and pyridine and heated at 70 °C for 2 h. The extracts were reduced to dryness, re-dissolved and spiked with internal standard mixture for quantification as mentioned above.

The samples were analysed on an Agilent 6890N gas chromatograph (GC) interfaced to a 5973 MSD mass spectrometer (MS) with a DB-5 (5% phenyl methyl siloxane) fused silica capillary column (30 m length, 0.25 mm inner diameter, 0.25 µm film thickness) at Linköping University, Sweden. The injector was operated in splitless mode at 300 °C and 1 µl of the extract was injected. The GC oven temperature was programmed for efficient separation of fatty acids and neutral lipids (*n*-alkanes, *n*-alkanols and sterols) and run separately (Ghosh et al., 2015). The MS was operated at 70 eV under full scan mode (*m/z* 40–600) and compounds in the samples were identified based on their retention times and fragmentation patterns and compared with their respective fragmentograms in the NIST MS Library (Version 2.0) and The Lipid Web (Christie, 2018). The *n*-alkane standard S4066 from CHIRON containing $C_{14} - C_{32}$ alkanes) was injected after every 10 samples to detect the instrument stability or drift in retention times. One sample blank was also analysed after every 10 samples to detect contamination during the analytical procedure.

Quantification of the biomarkers was done relative to the peak area of deuterated androstane used as internal standard. Carbon preference index (CPI), average chain length (ACL), and aquatic plant index ($P_{aq}$) were calculated to identify different OM sources and alteration (Poynter and Eglinton, 1990; Meyers and Ishiwatari, 1993; Ficken et al., 2000).

$$\mathrm{CPI_{alkane}} = 0.5\left[\frac{\Sigma(C_{25}-C_{33})_{\mathrm{odd}}}{\Sigma(C_{24}-C_{32})_{\mathrm{even}}} + \frac{\Sigma(C_{25}-C_{33})_{\mathrm{odd}}}{\Sigma(C_{26}-C_{34})_{\mathrm{even}}}\right] \quad (1)$$

$$\mathrm{ACL}(n-\mathrm{alkane}) = (\Sigma[\mathrm{Ci}]\times \mathrm{i})/\Sigma[\mathrm{Ci}];\mathrm{i} = \mathrm{Cnumber}23-33 \quad (2)$$

$$P_{aq} = \frac{C_{23}+C_{25}}{C_{23}+C_{25}+C_{29}+C_{31}} \quad (3)$$

 

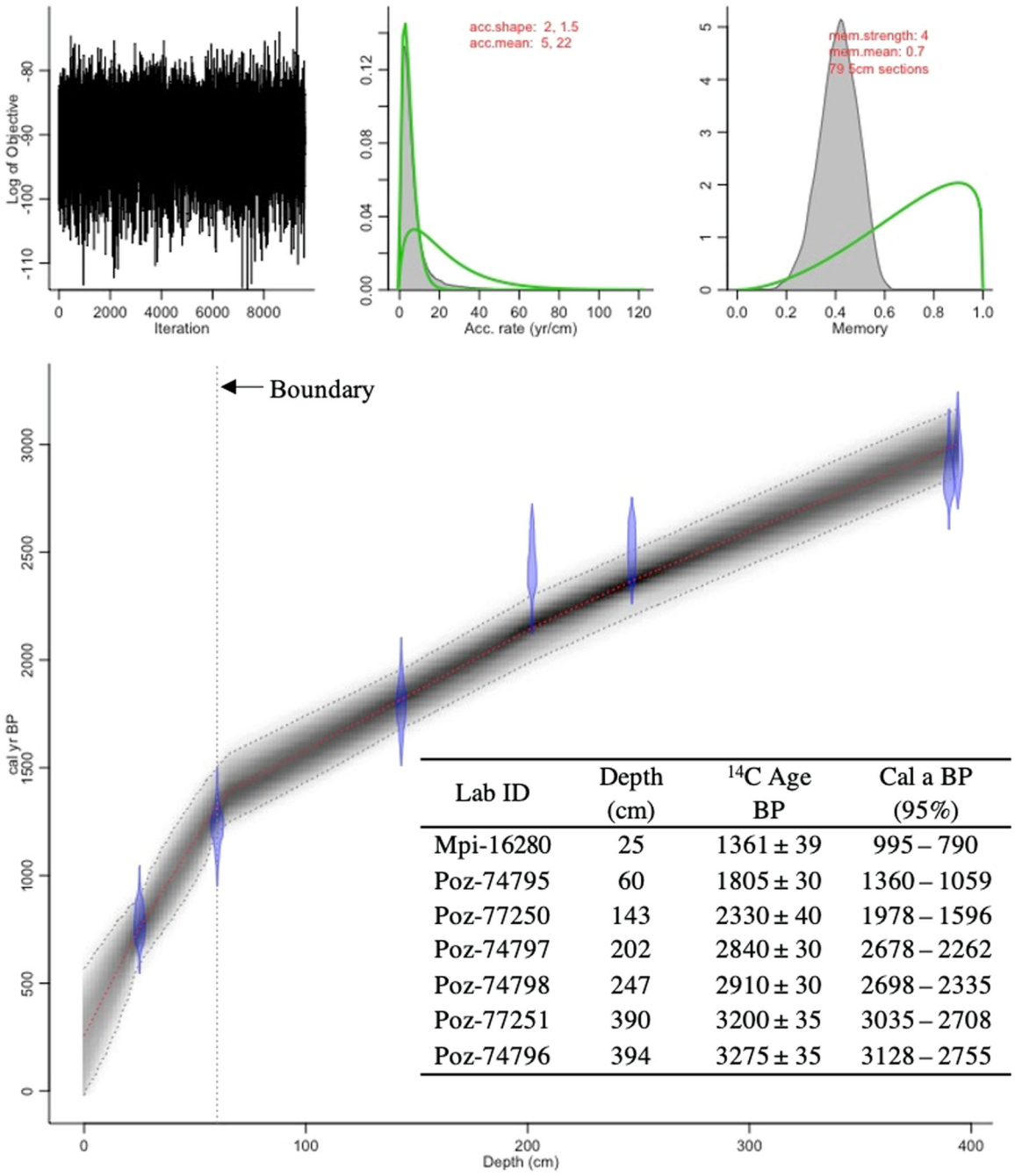


| Lab ID | Depth (cm) | $^{14}$C Age BP | Cal a BP (95%) |
|---|---|---|---|
| Mpi-16280 | 25 | 1361 ± 39 | 995 – 790 |
| Poz-74795 | 60 | 1805 ± 30 | 1360 – 1059 |
| Poz-77250 | 143 | 2330 ± 40 | 1978 – 1596 |
| Poz-74797 | 202 | 2840 ± 30 | 2678 – 2262 |
| Poz-74798 | 247 | 2910 ± 30 | 2698 – 2335 |
| Poz-77251 | 390 | 3200 ± 35 | 3035 – 2708 |
| Poz-74796 | 394 | 3275 ± 35 | 3128 – 2755 |

**Figure 2.** Revised age–depth model for the Bolgoda Lake, Sri Lanka. [Color figure can be viewed at wileyonlinelibrary.com]

## *Compound-specific carbon isotope analysis*

Stable carbon isotope ($\delta^{13}C$) analysis of individual *n*-alkanes (*n*-$C_{15}$ to *n*-$C_{33}$) was performed using a coupled gas chromatograph isotope ratio mass spectrometer (GC-IRMS) system equipped with a 7890A gas chromatograph (Agilent Technologies, Palo Alto, USA) and Delta V Plus Isotope Ratio Mass Spectrometer (Thermo Fisher Scientific, Bremen, Germany) at the Max Planck Institute for Biogeochemistry, Jena, Germany. The GC was equipped with a DB1-MS column (30 m length, 0.25 mm inner diameter, 0.25 mm film thickness). The injector was operated in splitless mode at 280 °C and 2 µl of the extract was injected. The GC oven was maintained in accordance with a temperature programme for efficient separation. Each sample was measured in triplicate with a mixture of $C_{15}$ to $C_{33}$ *n*-alkane standard mixture of known isotopic composition after every sample (three GC injections). Only peaks with an amplitude >150 mV were used for evaluation. The values were converted to the Vienna Pee Dee Belemnite (V-PDB) scale using the *n*-alkane standard mixture (offset correction). In addition, drift corrections were applied, determined by standards after every sample (Werner and Brand, 2001). The standard deviation of replicate measurements for all peaks in the standard mixture was 1.2‰.

## *Pollen analysis*

Pollen analysis is time-consuming and it needs a large amount of sample material. Hence, 16 samples were selected from key intervals distributed in the four palaeoclimate zones originally proposed in Gayantha et al. (2017) to support the biomarker-based interpretation and provide a general overview of the vegetation cover in specific intervals. Laboratory treatment of samples followed standard protocols (Fægri et al., 1989; Moore et al., 1991) with some additional modifications

 

(see Anupama et al., 2014) in the Laboratory of Palynology & Paleoecology, French Institute of Pondicherry, India. The mounted slides were observed under a light microscope (Olympus CHK) using 50x objective and the pollen samples were identified and enumerated. The Thanikaimoni pollen slide collection at the French Institute of Pondicherry and the regional pollen floras formed the basis for identification. Principal component analysis (PCA) was performed to ordinate pollen data and identify the dominant vegetation patterns using the statistical software package Canoco 5 for Windows (Microcomputer Power, NY, USA). Pollen taxa >3% in any sample was selected for the PCA.

## Results

### Chronology and climate zones

The revised age model did not change the suggested dates in Gayantha et al. (2017) significantly but provided reliable information for the section between 60 and 0 cm, which was earlier extrapolated with uncertainty. According to the revised age–depth model, the core revealed a depositional history of ~3000 cal a BP; the reservoir effect correction was calculated as 133 ± 65 years. This core was divided into four main climate zones based on the bulk geochemical proxies presented in Gayantha et al. (2017) and the new data in this study. These zones were identified as Zone 1 (2960–2390 cal BP), Zone 2 (2390–1800 cal a BP), Zone 3 (1800–1318 cal a BP) and Zone 4 (1318 cal a BP – present) that explain climate variability and changes in vegetation pattern and sedimentation rate.

### Biomarker trends and ratios of n-alkanes

The Bolgoda sediment core was characterised by a significant presence of long-chain *n*-alkanes, *n*-alkanols and *n*-alkanoic acids. *n*-Alkanes and *n*-alkanols had a unimodal distribution, whereas *n*-alkanoic acids indicated a bimodal distribution (Fig. 3). The *n*-alkanes were dominated by the odd-number homologues of *n*-$C_{29}$, $C_{31}$ and $C_{33}$, whereas *n*-alkanols and *n*-alkanoic acids were dominated by even-chain *n*-$C_{26}$, $C_{28}$ and $C_{30}$ homologues. $C_{31}$ was the dominant *n*-alkane, whereas $C_{28}$ and $C_{26}$ peaks were dominant for alkanols and alkanoic acids, respectively (Fig. 3 and Appendix 2). Variability in the *n*-alkane indices was more clearly distinct relative to *n*-alkanols and *n*-alkanoic acids (see Appendix 2), and therefore *n*-alkanes were pursued for compound-specific isotope analysis (CSIA).

$P_{aq}$ (for *n*-alkanes) showed a generally low average value of 0.19 and ranged from 0.08 to 0.47. $P_{aq}$ reached its maximum value at 227 cm and showed two clear peaks at 240–215 cm and 172–150 cm. $P_{aq}$ again increased at 15–0 cm (Fig. 4). The ACL for *n*-alkanes showed an opposite trend to $P_{aq}$. The ACL values ranged between 30.6 and 28.2 with a core average of 29.8. At 385–252 cm (Zone 1) and 160–140 cm (Zone 3) ACL showed higher values. At the end of Zone 4 (from 15 cm to the top of the core), ACL showed a clear decline. CPI values for *n*-alkanes were generally high (average 3.1) and ranged between 1.3 and 4.3 with a strong odd/even predominance. The odd/even predominance was more prominent for long-chain *n*-alkanes than the short-chain *n*-alkanes. At 377–252 cm and 140–70 cm, CPI values were elevated with a core upward increasing trend (Fig. 4).

### Triterpenols

Taraxerol was the most abundant triterpenol identified. In addition, β-amyrin, lupeol, and germinicol were identified in the sediment core, though they occurred at lower abundances. Taraxerol content ranged from 58 ng/mg total organic carbon (TOC) to 985 ng/mg TOC; the highest concentration of taraxerol occurred from 366 to 379 cm. From 252 to 202 cm the core showed an upward increasing trend and reached a value of 836 ng/mg TOC at 202 cm (Fig. 4). β-Amyrin was the second most abundant triterpenol and ranged between 217 and 17 ng/mg TOC. Lupeol ranged between 2 and 31 ng/mg TOC. Germinicol was the least abundant triterpenol and ranged between 13.7 and 1.9 ng/mg TOC. The relatively less abundant triterpenols displayed generally similar trends like taraxerol.

### $\delta^{13}C$ isotopes in n-alkanes

$\delta^{13}C$ isotopes of *n*-$C_{33}$, *n*-$C_{31}$ and *n*-$C_{29}$ alkanes were selected because the $^{13}CO_2$ peaks of these *n*-alkanes were detected more evenly throughout the core. The long-chain *n*-$C_{33}$, $C_{31}$ and $C_{29}$ alkanes had average $\delta^{13}C$ values of -32.3‰, -33.5‰, and -32.2‰, respectively. The $\delta^{13}C$ trends for $C_{31}$ and $C_{33}$ *n*-alkanes showed generally similar patterns. In Zone 1, $\delta^{13}C_{C33}$ and $\delta^{13}C_{C31}$ were higher in the beginning and gradually decreased up the core until 252 cm. Between 252 cm and 202 cm, $\delta^{13}C_{C33}$ showed a clear and rapid core upward increasing trend, which reached the maximum value (−27.3‰) at around 202 cm. Between 160 cm and 140 cm, $\delta^{13}C_{C33}$ and $\delta^{13}C_{C31}$ indicated a short deviation (higher values) and $\delta^{13}C_{C31}$ reached its maximum value of -31.7‰. From 140 cm to 60 cm both $\delta^{13}C_{C33}$ and $\delta^{13}C_{C31}$ showed a decreasing trend. From 60 cm to the top of the core (Zone 1), $\delta^{13}C$ values of long-chain *n*-alkanes ($C_{29}$, $C_{31}$ and $C_{33}$) increased towards the top of the core. $\delta^{13}C_{C29}$ values showed a narrow fluctuation around its mean value (−32.2‰) except between 252 and 202 cm where low values were clearly indicated (−33.1‰; Fig. 4).

### Pollen

We identified 100 different pollen taxa in the Bolgoda sediments (see Appendices 3 and 4 for complete pollen taxa). These included *Mallotus*, *Phoenix*, *Syzygium*, *Areca* and Arecaceae, representative of trees in tropical dry evergreen forests (TDEF), and others, such as *Ixora*, *Randia*, Rutaceae and *Ziziphus* that represent woody shrubs. The pollen taxa Rhizophoraceae and Avicenniaceae are representative of mangrove vegetation, with the former being generally more abundant throughout the core. Both TDEF and mangrove pollen counts fluctuate throughout the core. Grasses were not differentiated beyond the family level (Poaceae) and in any case, they constitute the most consistently represented pollen taxon in these sediments (18–42%). *Pandunus*, *Typha* and *Cyperacea* pollen taxa represent a (freshwater) aquatic environment and occur in a consistently low proportion throughout the core (Fig. 6).

According to the PCA, principal component axes 1 and 2 account for 60% of the variation in pollen taxa. PC1 showed positive scores with *Ixora*, *Phoenix*, *Areca/Pinanga*, Avicenniaceae, *Randia* and *Syzygium* and negative scores with Arecaceae, *Mallotus* and *Macarang*. Grasses and sedges indicated positive scores with PC2, whereas Rhizophoraceae, Rutaceae, *Cocos* and *Phyllanthus* showed negative scores (Fig. 7). PCA indicates that Avicenniaceae mangrove correlates well with dry/deciduous forest pollen taxa in contrast to Rhizophoraceae. The Bolgoda pollen data revealed three mangrove zones. The zone extending from 365 to 290 cm was dominated by Rhizophoraceae; 200–250 cm was dominated with Avicenniaceae; and 10–25 cm consisted of Rhizophoraceae

 

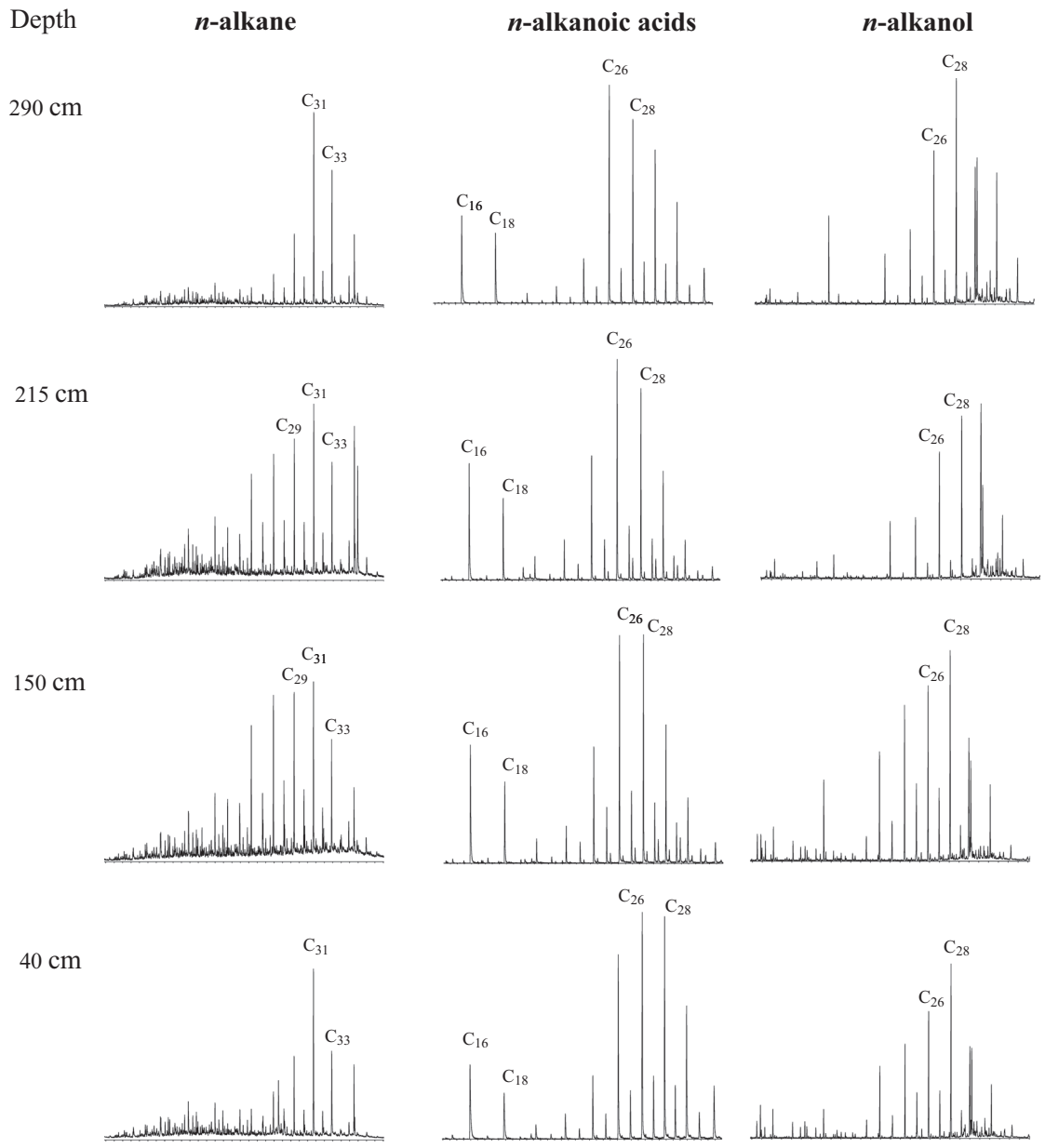


**Figure 3.** Gas chromatography–mass spectrometry chromatograms of *n*-alkanes, *n*-alkanoic acids, and *n*-alkanols for selected depths in Bolgoda Lake, Sri Lanka.

along with *Pandunus* – an aquatic freshwater taxon. *Pandunus* was also identified between 150 and 170 cm in the Bolgoda sediment core (Fig. 6).

## Discussion

### *Palaeoenvironmental implications*

Although the 4.1 m long sediment core from Bolgoda Lake only captures the Late Holocene period (~3000 yrs BP), the rapid sedimentation rate in the study area facilitates high-resolution reconstruction of palaeoclimate and palaeoenvironmental records for South Asia beyond the Indian sub-continent. The revised BACON model marks a boundary at 60 cm depth identifying two significantly different sediment accumulation rates below and above this boundary (Fig. 2).

In this study, we consider only the depths from 385 to 0 cm for biomarker interpretation since core depth below 385 cm consisted of weathered bedrock and the OM content was too low to produce a reliable record. The distribution of *n*-alkanes in the Bolgoda sediments shows predominantly long-chain monomers (Fig. 3) that imply dominant contributions of allochthonous OM and/or preferential degradation of short-chain monomers after deposition (Meyers, 2003).

The dominance of the *n*-$C_{31}$ alkane, followed by *n*-$C_{33}$, throughout the core (Fig. 3), as well as the abundance of pollen belonging to Poaceae (Fig. 6), indicates that grass was the major vegetation cover in the catchment and became the major source of OM input throughout the Late Holocene. The positively correlated pollen taxa in PC1 mainly represent woody plants dominant in tropical dry areas and include trees (*Syzygium*, *Areca*), woody shrubs (*Randia*, *Ixora*), and mangroves (Avicenniaceae; Fig. 7). Pollen belonging to shrubs adapted to aridity and Avicenniaceae mangrove showed a negative correlation with grasses, sedges and *Mallotus*, *Macaranga* and Arecaceae trees (Fig. 7), which prefer higher precipitation. This observation indicates the adaptation of vegetation in response to changing climatic conditions.

 

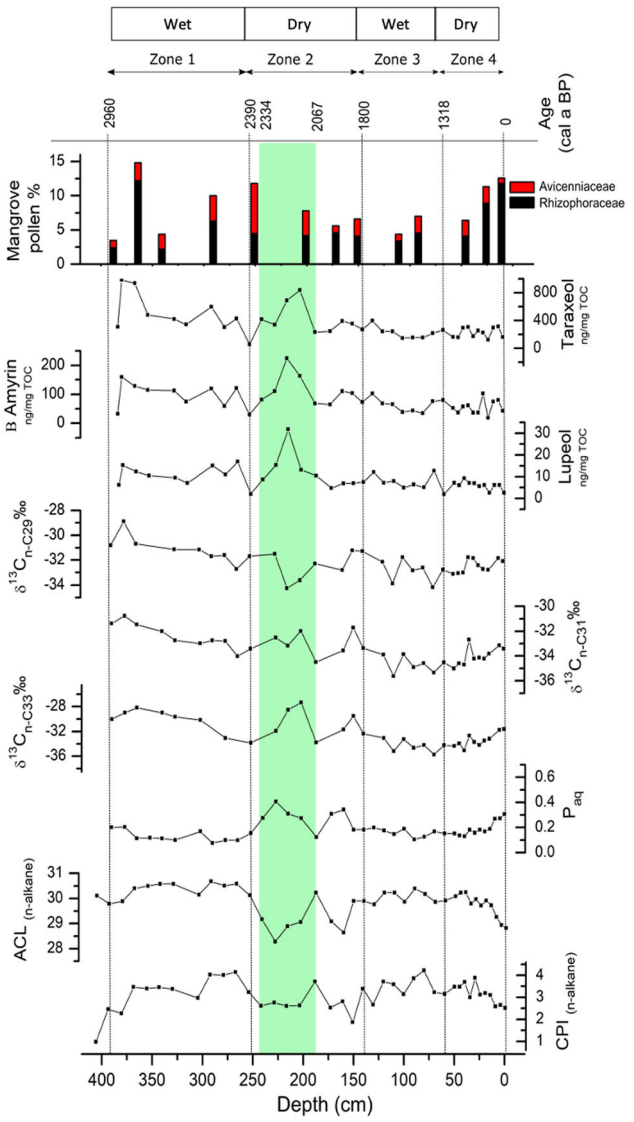


**Figure 4.** Trends of mangrove pollen percentages, triterpenols (taraxerol, β-amyrin, and lupeol), carbon isotope values ($\delta^{13}C‰$) of *n*-$C_{29}$, *n*-$C_{31}$ and *n*-$C_{33}$ alkanes, aquatic plant index ($P_{aq}$), average chain length (ACL) and carbon preference index (CPI) of *n*-alkanes in Bolgoda Lake, Sri Lanka. [Color figure can be viewed at wileyonlinelibrary.com]

## *Mangrove vegetation, palaeosalinity changes and droughts*

Salinity in Bolgoda Lake is mainly controlled by seasonal variations in the IOM system rather than sea-level changes (Ratnayake et al., 2018). Moreover, existing limnological studies have reported that the sea level around Sri Lanka has been relatively stable during the last ~3000 yrs BP (Ranasinghe et al., 2013). Hence, proliferation of mangroves interpreted based on different proxies in the Bolgoda Lake record requires an explanation. Salinity and sediment characteristics (i.e. waterlogged inter-tidal conditions) are two main factors that control the growth of mangroves and their survival (Kumaran et al., 2005; Ranawana, 2017). The abundance of mangroves is thus an indication of high salinity and stagnant conditions in the lake. These conditions are likely a product of increased seawater intrusion and reduced freshwater input during periods of low precipitation. During periods of high precipitation, the lake became less saline due to high freshwater input that reduced the mangrove cover (e.g. Parida and Jha, 2010; Setyaningsih et al., 2019). Thus our study provides a new set of proxy data, and a novel methodological approach for determining aridity and salinity changes in tropics where mangrove vegetation is, or has been, present.

Mangrove pollen and various triterpenols act as proxies for tracking the changing abundance of mangrove vegetation around Lake Bolgoda and the associated shifts in environmental and hydrological conditions. Triterpenols identified in this core (i.e. taraxerol, β-amyrin, lupeol and germinicol) are mangrove-specific biomarkers (Versteegh et al., 2004; Ranjan et al., 2015; Ratnayake et al., 2017). According to the pollen data, Rhizophoraceae and Avicenniaceae are the two major mangrove pollen taxa in the Bolgoda core. Notably, Avicenniaceae are highly salt tolerant and can survive under a wide range of salinities. In addition, Avicenniaceae also thrive under arid conditions (Goldstein and Santiago, 2016). Therefore, the dominance of Avicenniaceae over Rhizophoraceae pollen counts will indicate a significant increase in lacustrine salinity and arid conditions.

Furthermore, the CSIA analysis of *n*-alkanes provides additional source-specific information regarding palaeoenvironmental conditions. Differences in the distribution of long-chain *n*-alkanes in different types of vegetation can be observed (e.g. mangroves and grasses; Ratnayake et al., 2019). Normally, tropical grasses tend to dominate in long-chain *n*-alkanes such as $C_{31}$, $C_{33}$ and $C_{35}$ (Garcin et al., 2014 and see also Fig. 5). Consistent with this trend, *n*-$C_{31}$ and *n*-$C_{33}$ alkanes show a very strong correlation coefficient ($r = 0.99$) implying a common origin (Appendix 1). Therefore, tropical grasses growing in the catchment are probably the main source of $C_{31}$ and $C_{33}$ *n*-alkanes (e.g. Meyers, 2003; Garcin et al., 2014). Despite the slight variation between different species, mangrove-derived OM is typically dominated by *n*-$C_{29}$ (mangrove leaves) and *n*-$C_{23}$ (mangrove wood) alkanes (He et al., 2017; Ratnayake et al., 2019). Consistent with this line of evidence, both taraxerol and β-amyrin which are diagnostic for mangroves, showed the highest correlation with *n*-$C_{29}$ and *n*-$C_{23}$ alkanes and this further supports the interpretation about OM sources and their variability.

The $\delta^{13}C_{C33}$ record shows positive correlation with taraxerol ($r = 0.70$, $p < 0.01$) and β-amyrin ($r = 0.61$, $p < 0.01$). However, $\delta^{13}C_{C31}$ shows a weak positive correlation with taraxerol ($r = 0.44$, $p < 0.01$) and β-amyrin ($r = 0.32$, $p = 0.09$) (Fig. 8). Additional contributions of *n*-$C_{31}$ alkanes from a variety of other sources perhaps explains the patterns. This observation implies that grasses (represented by *n*-$C_{33}$ alkanes) have higher $\delta^{13}C$ values during periods with low precipitation that resulted in high lake salinity, as inferred by dense mangrove vegetation around the lake. Notably, tropical plants behave in two different ways to survive during arid conditions or droughts. Many terrestrial plants, including grasses, show isohydric behaviour, which is closing of the stromata to minimise water loss at the expense of reduced $CO_2$ intake (Goldstein and Santiago, 2016). However, mangrove vegetation possesses special adaptations to extract freshwater from saline water, and demonstrates anisohydric behaviour, i.e. opening of the stromata to gain more $CO_2$ at the expense of losing water (Nguyen et al., 2017). This adaptation results in lower $\delta^{13}C$ values during periods of aridity, providing yet another proxy for more saline and arid conditions in sporadic mangrove-dominated settings. This different arid/drought surveillance adaptation in vegetation can cause shifts in $\delta^{13}C$ values in sediment records that can be precisely identified by their dominant *n*-alkane $\delta^{13}C$ values (Douglas et al., 2012).

## *Palaeoclimate and palaeoenvironmental reconstruction*

The four zones identified in the Bolgoda Lake core based on $^{14}C$ chronology and different proxies, including those

 

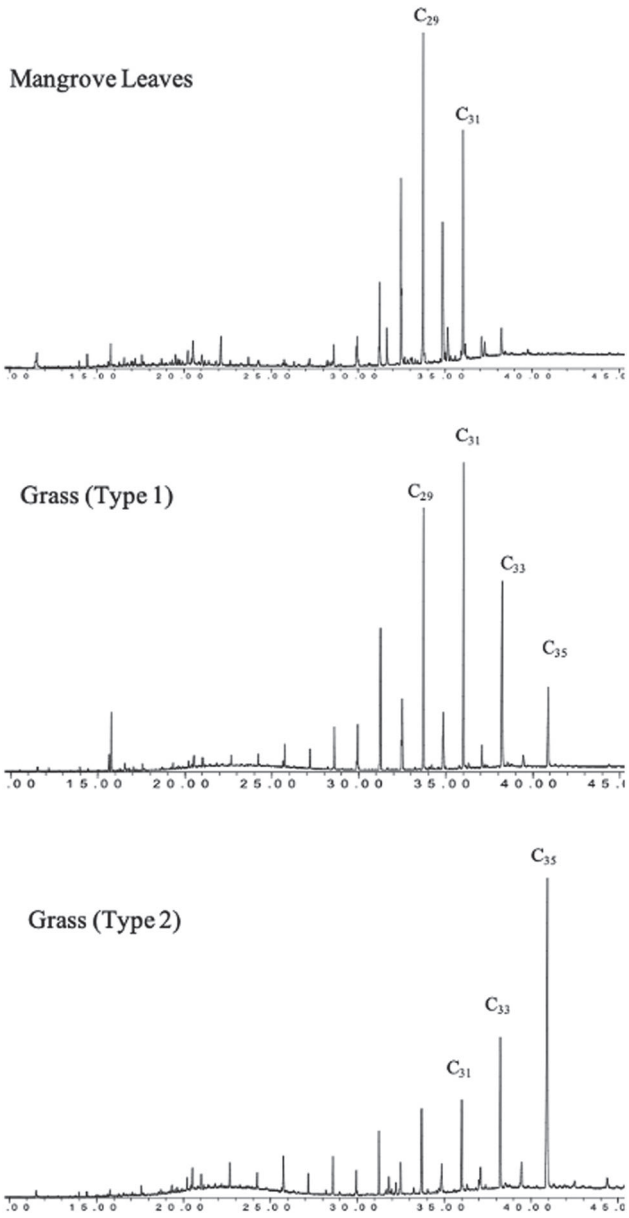


**Figure 5.** *n*-Alkane distribution of main organic matter sources (mangrove and grasses) in Bolgoda Lake catchment.

developed for determining the preponderance of mangrove taxa, trace the catchment responses to variation in IOM intensity during the Late Holocene.

## *Zone 1 (2960 to 2390 cal a BP; 385–252 cm)*

This zone is dominated by allochthonous OM input from the catchment according to biomarker trends. High CPI values (average = 3.4, standard deviation (SD) = 0.6) and ACL (average = 30.4, SD = 0.3) of *n*-alkanes together with low $P_{aq}$ values (average = 0.13, SD = 0.04) in this zone suggest a limited contribution of all types of macrophytes and enhanced input of land-derived OM (Fig. 4). These high values are most likely due to intense rainfall leading to dense terrestrial vegetation as well as high freshwater input from streams delivering terrestrially sourced OM into the lake. According to the pollen diagram, Zone 1 is mainly dominated by grasses and sedges, together with trees of wet evergreen forests like *Mallotus*, Arecaceae and *Macaranga* (Fig. 6). Rhizophoraceae are the dominant mangrove vegetation and their pollen occurs in high numbers (Fig. 4). This points to relatively low salinity and mild environmental conditions.

Biomarker proxies (triterpenols) indicate that Zone 1 is rich in mangrove-derived OM with a higher abundance of taraxerol (average = 486 ng/mg TOC), β-amyrin (average = 95 ng/mg TOC), and lupeol (11 ng/mg TOC) (Fig. 4). Towards the beginning of this period, an increase of taraxerol can be interpreted as dense mangrove vegetation. After this, taraxerol shows a decreasing trend. Consistent with these trends, $\delta^{13}C$ values of grass-derived *n*-$C_{33}$ (and partially *n*-$C_{31}$) alkanes (average = 29.9‰; SD = 1.8 and average = −32.4‰; SD = 1.0, respectively) show elevated values during the beginning of this period with a decreasing trend over time (Fig. 4). With increasing rainfall and wet conditions, grasses take up atmospheric $CO_2$ and freely open their stromata, leading to a decrease in the $\delta^{13}C_{C33}$ values. Together, these proxies suggest an increase of freshwater recharge into the lake and wet conditions, implying a high intensity of IOM in Zone 1.

## *Zone 2 (2390 to 1800 cal a BP; 252–140 cm)*

Several diagnostic biomarker trends can be distinguished in Zone 2 that trace the OM source inputs and palaeoenvironmental conditions in Bolgoda Lake and its catchment. The decrease in land-derived OM supply can be observed as indicated by biomarker signals and pollen data. Two excursions of $P_{aq}$ values can be identified between 2334 and 2216 cal a BP (240–215 cm) and between 1981 and 1856 cal a BP (172–150 cm), which indicate significant input of lacustrine OM into the lake (Fig. 4). This observation is also supported by the appearance of pollen belonging to the aquatic plant taxa *Pandunus* and *Typha* between 1971 and 1856 cal a BP (170–150 cm; Fig. 6).

The period between 2267 and 2061 cal a BP (226–186 cm) is characterised by elevated values of triterpenols, signifying the presence of dense mangrove vegetation around the lake. The notable dominance of Avicenniaceae over Rhizophoraceae pollen indicates that high salinity and arid/drought-like conditions prevailed in the catchment (Fig. 4). In addition, shrubs of *Randia* and *Ixora*, characteristic of arid environments, are also common in this section. Arid conditions are further supported by the $\delta^{13}C$ values of $C_{33}$ and $C_{29}$ *n*-alkanes. The *n*-$C_{33}$ alkanes mainly derived from grasses show higher, arid-stressed $\delta^{13}C$ values. Due to the abundance of mangrove vegetation during this period, and less input of land-derived OM as a result of low stream recharge, the *n*-$C_{29}$ alkanes are derived dominantly from mangroves that have lower $\delta^{13}C_{C29}$ values under conditions of increased aridity (Fig. 4).

The period extending from 2067 to 1800 cal a BP (187–140 cm) is characterised by a decrease in triterpenols and $\delta^{13}C_{C33}$ values, indicating a decline of mangrove vegetation and termination of the drought. Consistent with this trend, the emergence of *Pandunus* and *Typha* in this sub-zone supports more freshwater input into the lake. In addition, grasses and sedges (Poaceae and Cyperaceae) increase again. Overall, this zone is characterised by abrupt changes of climate and environmental conditions.

## *Zone 3 (1800 to 1318 cal a BP; 140–60 cm)*

The biomarker proxies $P_{aq}$, ACL, and CPI for *n*-alkanes in Zone 3 show generally similar trends to those seen in Zone 1 (Fig. 4). Low $P_{aq}$ values (average = 0.16, SD = 0.03) with high ACL (average = 30, SD = 0.2) and CPI values (average = 3.5, SD = 0.5) of *n*-alkane indicate that this period is characterised by a high input of land-derived terrestrial plants, and limited contributions from autochthonous aquatic plants. In addition, $\delta^{13}C_{C33}$ and $\delta^{13}C_{C31}$ alkanes show more negative values

 

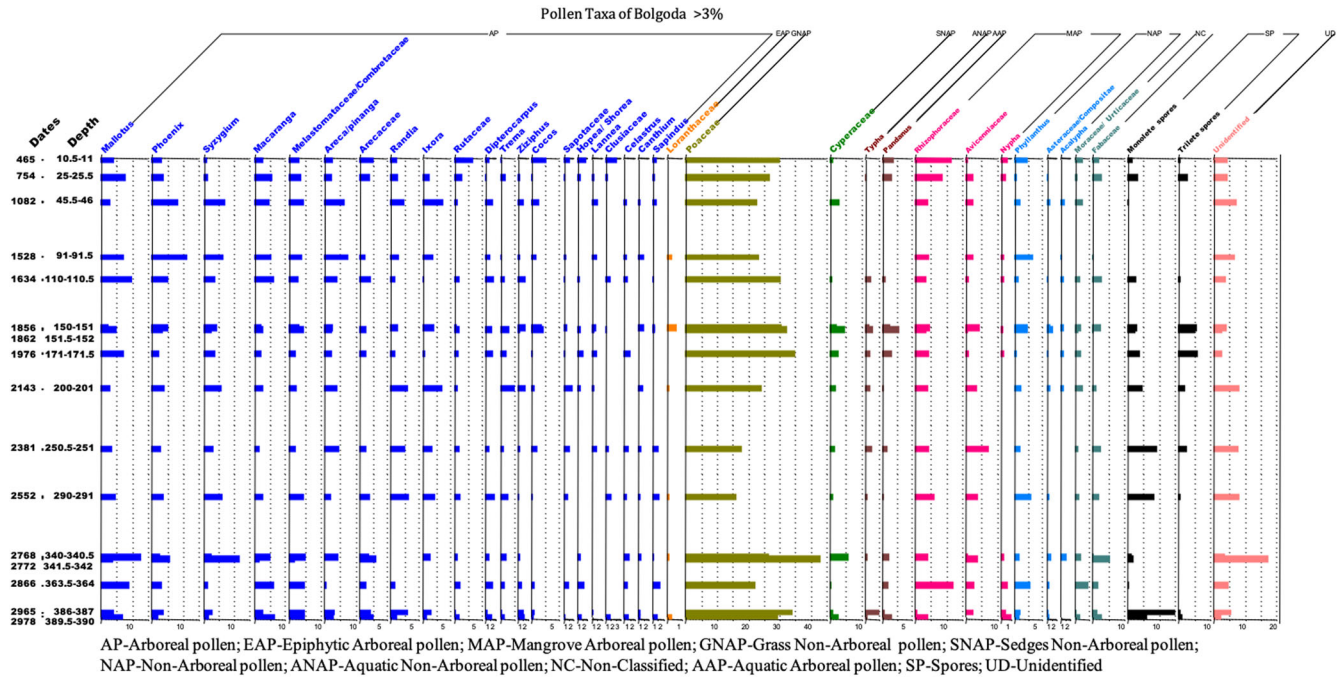


**Figure 6.** Pollen diagram of Bolgoda Lake (pollen taxa contains more than 3% in any sample are shown here). [Color figure can be viewed at wileyonlinelibrary.com]

(average = −34.1‰; SD = 1.2 and average -34.5‰; SD = 0.8, respectively), implying wet conditions (Fig. 4). In contrast to Zone 1, however, Zone 3 shows a clear decline in mangrove-derived triterpenols (average values of taraxerol = 228 ng/mg TOC, β-amyrin = 63 ng/mg TOC, lupeol = 8 ng/mg TOC). According to the mangrove pollen data, both Rhizophoraceae and Avicenniaceae pollen are present in relatively low numbers in this zone. However, Rhizophoraceae are more abundant than Avicenniaceae (Fig. 4). The results imply that mangrove vegetation around the lake was sparse. This period was least favourable for the proliferation of mangroves, possibly due to increased freshwater supply and less stagnation in the water body. Consistent with this, the period was dominated by trees characteristic of wet evergreen forests, including *Areca*, *Mallotus*, *Macaranga*, *Phoenix* and *Syzygium* in the catchment. While the catchment has an abundance of major trees, mangrove vegetation is relatively low during this period. Thus, this zone is suggested to have a strong IOM intensity and overall wet conditions.

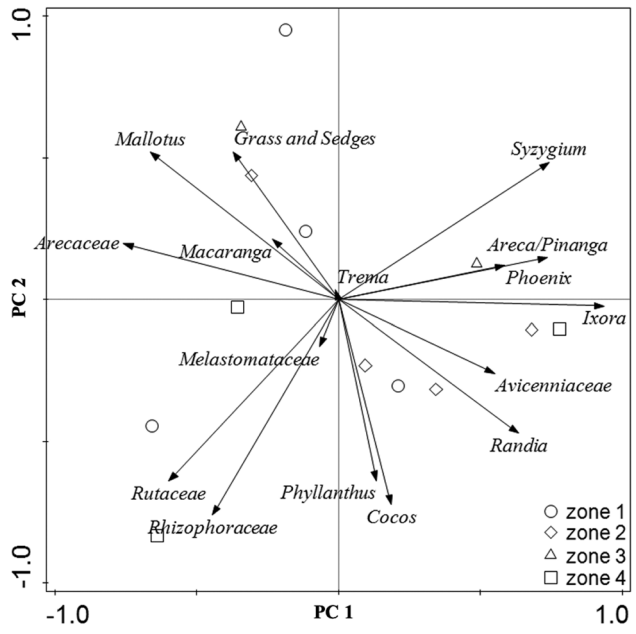


**Figure 7.** Principal component analysis biplot for selected pollen taxa (>3%) in Bolgoda Lake.

## *Zone 4 (1318 cal a BP to present; 60–0 cm)*

In this zone, *n*-alkane ACL (average = 30, SD = 0.5) and CPI (average = 3.2, SD = 0.4) values are high, with a decreasing trend up the core, implying a decline in the supply of land-derived OM. In contrast to this trend, $P_{aq}$ values (average = 0.19, SD = 0.06) increase up the core c. 566 cal a BP to the present (15–0 cm). From 566 cal a BP to present (15–0 cm), *n*-alkane ACL and CPI show a clear decline in their values, implying an increase in the contribution from macrophytes in the lake (Fig. 4). Therefore, the period between 1318 and 566 cal a BP (60–15 cm) can be considered as one dominated by the input of more allochthonous OM. In contrast, the top part of the core (15–0 cm, 566 cal a BP – present) is characterised by an enhanced contribution of autochthonous OM.

The pollen data indicate that Rhizophoraceae dominate alongside an increase in *Pandunus* during the period 754–465 cal a BP (25–10 cm; Fig. 6). However, relatively low concentrations of mangrove-specific triterpenols contradict the information provided by pollen data, especially between 754 and 465 cal a BP (25–10 cm). Notably, the low accumulation rate in Zone 4 introduces a bias resulting in high pollen counts and may not reflect the true information about the vegetation cover. Therefore, we rely mostly on the biomarker and stable isotope records in this zone to reconstruct the palaeoenvironmental changes. Despite the fact that mangrove-derived triterpenols show only a slight increase in Zone 4, $\delta^{13}C_{C33}$ and $\delta^{13}C_{C31}$ measurements show a clear increasing trend (average = −33.5‰, SD = 1.1 and −34.0‰, SD = 0.7, respectively), suggesting dry conditions in the catchment (Fig. 4). Zone 4 generally represents a wet period with a weakening in rainfall intensity from 754 cal a BP towards the present that is validated by instrumental records for the last century obtained from the western slopes of the highlands (de Silva and Sonnadara, 2016).

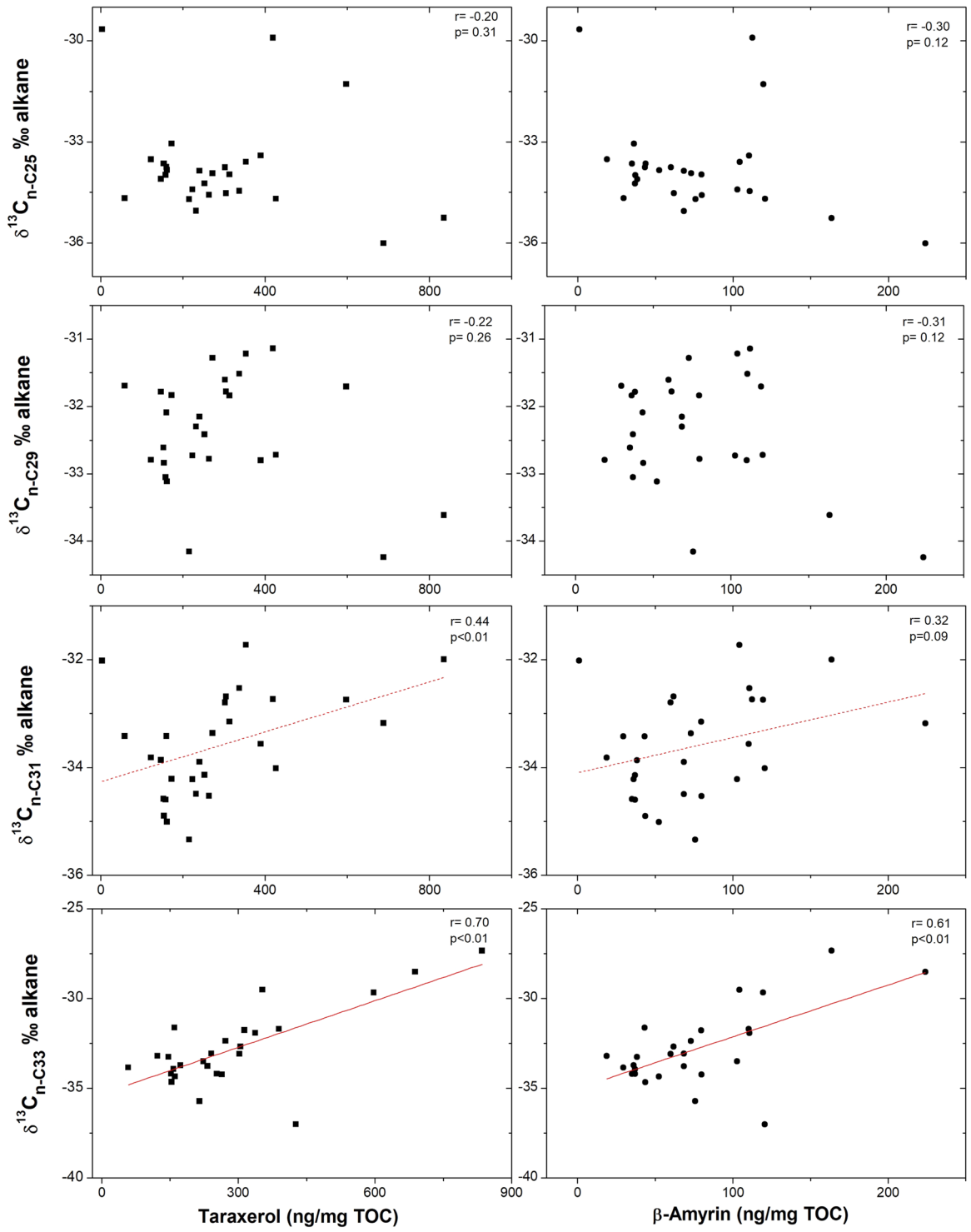


**Figure 8.** Correlation between major triterpenols (taraxerol and β-amyrin) and carbon ($\delta^{13}C‰$) isotope values of *n*-$C_{25}$, *n*-$C_{29}$, *n*-$C_{31}$ and *n*-$C_{33}$ alkane. [Color figure can be viewed at wileyonlinelibrary.com]

## *South Asian comparisons and potential human implications*

The palaeoclimatic and palaeoenvironmental shifts observed in the Bolgoda Lake record align with observations from other climate archives for Late Holocene changes in South Asia. Significantly, aridity noted in Zone 2 between 2334 and 2061 cal a BP, closely correlates with a record based on pollen and microfossils reported in Kodina, India, that is located in the core monsoon region (Farooqui et al., 2013). In addition, regional records including the peat deposit from Horton plains (Premathilake and Risberg, 2003), Pookode Lake (Veena et al., 2014) and Lonar Lake (Prasad et al., 2014) show a climatic transition from wet to dry conditions around 2000 yrs BP (also see comparison of regional Late Holocene climate records in Gayantha et al., 2017). This correlation provides further support for the assertion that the increasing aridity, salinity and the growth of mangrove vegetation around Bolgoda Lake at this time are related to the weakening of the IOM, and that the Bolgoda Lake records palaeoenvironmental changes that reflect the IOM variability.Detailed regional reconstruction of IOM fluctuations and their impacts on environments will potentially enable the more effective

 

association of palaeoenvironmental data with that derived from archaeology and history. In a broader South Asian context, fluctuations in aridity, notably between 3000 and 2000 years ago on the Indian sub-continent, have been associated with changing Iron Age subsistence and settlements in arid regions such as the southern Deccan (1200–300 BC; Ponton et al., 2012; Roberts et al., 2015), that encouraged sedentary populations to congregate near reliable watercourses (1200–300 BC; Johansen, 2010; Bauer, 2014), and more mobile strategies to flourish elsewhere (Roberts et al., 2015). In a Sri Lankan context, there remains a question as to whether the rise and fall of the UNESCO world heritage sites of Anuradhapura (c. 2500–1000 years ago) and Polonnaruwa (c. 900–700 years ago) were associated with responses to a variable IOM in a part of the island prone to prolonged droughts (Gilliland et al., 2013).

In general, the Bolgoda Lake record seems to suggest that the wet zone of Sri Lanka was relatively resilient to changes in the IOM observed elsewhere, particularly between 3000 and 2000 years ago. We do identify clear increases in aridity and a reduction in IOM intensity in Zone 2 (between 2334 and 2061 cal a BP), correlating to the written historical records in Sri Lanka (*Mahavansha*, *Sihalavatthu Pakarana*) that refer to *Beminitiya Saaya*, or the Great Famine, which occurred at the end of the first century BC (between 103 and 89 BC) due to severe drought (Shaw and Nguyen, 2011). Similarly, a weaker IOM c. 1318–566 cal a BP in Zone 4 may have framed shifts in the political capital of Sri Lanka from Anuradhapura and Polonnaruwa in the northern dry zone towards the wet zone of Kandy (Lucero et al., 2015; Roberts, 2019). Yet, while the Bolgoda Lake record does show shifts in IOM intensity, the ultimate implications for the local environments seem to be relatively minor, with a constant input of freshwater and surrounding vegetation, which is perhaps what made the wet zone so attractive for growing populations from 900 AD onwards (Lucero et al., 2015). To properly test this hypothesis, however, a high-resolution, human-relevant palaeoenvironmental record is sorely needed from the north of Sri Lanka, given the highly divergent influences of the southwest and northeast monsoon in different parts of the island.

## Conclusions

Our study reconstructs ~3000 a BP of detailed palaeoclimate and palaeoenvironmental changes in the Bolgoda Lake catchment in southwestern Sri Lanka. Using multiple proxies, including a novel combination of proxies for mangrove abundance, we have been able to reconstruct the watershed vegetation, lake salinity changes and variation in OM source inputs. A combined analysis of these proxies reveals the fluctuation between wet and dry conditions alongside IOM intensity. Fluctuations in the IOM intensity critically influenced the salinity variation that led to changes in the type and density of associated mangrove vegetation. Grasses and some major trees demonstrate lower abundances in the catchment during periods of weak rainfall. Our study demonstrates that the compound-specific carbon isotope values of long-chain *n*-alkanes can be used to trace the fluctuations in aridity. However, it is very important to identify the dominant sources of specific *n*-alkanes, with the support of other proxies such as specific sterols (triterpenols) and/or pollen to correctly interpret the climate signals in Sri Lanka.

Our results indicate two key periods of monsoonal variation during the Late Holocene. From c. 3000 to 2400 cal a BP, precipitation increased, and its intensity strengthened. After that, the rainfall showed an overall weakening trend with rapid, abrupt changes between c. 2400 and 1800 cal a BP. These trends correlate both with other palaeoenvironmental records influenced by the IOM from South Asia and historically recorded ancient droughts in Sri Lanka, though more testing is required to determine the actual consequences of these precipitation shifts on human behaviour/settlements. After 1800–1300 cal a BP, rainfall apparently increased in the vicinity of Bolgoda Lake with a gradual weakening trend until the present.

## Supporting information

Additional supporting information may be found in the online version of this article at the publisher's web-site.

**Appendix 1:** Correlation coefficient of contents of long-chain n-alkanes and major triterpenols (taraxerol and β-amyrin) in Bolgoda Lake, Sri Lanka. Correlation is significant at the 0.01 level (2-tailed) is indicated in bold.

**Appendix 2:** Trends of terrestrial plant index ($\mathbf{P}_{wax}$), germinicol, **CPI** and **ACL** of *n*-alkanol and *n*-alkanoic acids and $\delta^{13}C_{C25}$ *n*-alkane in Bolgoda Lake, Sri Lanka.

**Appendix 3:** Entire pollen diagram of Bolgoda North Lake, Sri Lanka (Part 1)

**Appendix 4:** Entire pollen diagram of Bolgoda North Lake, Sri Lanka (Part 2)

*Acknowledgements.* KG thanks Lena Lundman, Susanne Karlsson, and Steffen Rühlow for technical support in the labs. G. Orukaimani and Panchala Weerakoon helped in the preparation of pollen slides. Markus Lunge helped in statistical analysis. Funding was provided by the Swedish Research Council to JR (Grant 2012-6239) and Max Planck Society.

## References

Anupama K, Prasad S, Reddy CS. 2014. Vegetation, land cover and land use changes of the last 200 years in the Eastern Ghats (southern India) inferred from pollen analysis of sediments from a rain-fed tank and remote sensing. *Quaternary International* **325**: 93–104.

Bauer AM. 2014. Impacts of mid- to late-Holocene land use on residual hill geomorphology: A remote sensing and archaeological evaluation of human-related soil erosion in central Karnataka, South India. *The Holocene* **24**: 3–14.

Blaauw M, Christen J. 2011. Flexible paleoclimate age-depth models using an autoregressive gamma process. *Bayesian Analysis* **6**: 457–474.

Christie W. 2018. Lipid Library https://www.lipidhome.co.uk/ms/others/others-arch/index1.htm

Douglas PMJ, Pagani M, Brenner M *et al.* 2012. Aridity and vegetation composition are important determinants of leaf-wax δD values in southeastern Mexico and Central America. *Geochimica et Cosmochimica Acta* **97**: 24–45.

Erdelen W. 1988. Forest ecosystems and nature conservation in Sri Lanka. *Biological Conservation* **43**: 115–135.

Fægri K, Kaland PE, Krzywinski K. 1989. *Textbook of pollen analysis*. John Wiley & Sons Ltd.

Farooqui A, Gaur AS, Prasad V. 2013. Climate, vegetation and ecology during Harappan period: Excavations at Kanjetar and Kaj, mid-Saurashtra coast, Gujarat. *Journal of Archaeological Science* **40**: 2631–2647.

Ficken KJ, Li B, Swain DL *et al.* 2000. An n-alkane proxy for the sedimentary input of submerged/floating freshwater aquatic macrophytes. *Organic Geochemistry* **31**: 745–749.

Fuller DQ, Boivin N, Korisettar R. 2007. Dating the Neolithic of South India: new radiometric evidence for key economic, social and ritual transformations. *Antiquity* **81**: 755–778.

Garcin Y, Schefuß E, Schwab VF *et al.* 2014. Reconstructing $C_3$ and $C_4$ vegetation cover using n-alkane carbon isotope ratios in recent lake sediments from Cameroon, Western Central Africa. *Geochimica et Cosmochimica Acta* **142**: 482–500.

 

Gayantha K, Routh J, Chandrajith R. 2017. A multi-proxy reconstruction of the late Holocene climate evolution in Lake Bolgoda, Sri Lanka. *Palaeogeography, Palaeoclimatology, Palaeoecology* **473**: 16–25.

Ghosh D, Routh J, Dario M *et al.* 2015. Elemental and biomarker characteristics in a Pleistocene aquifer vulnerable to arsenic contamination in the Bengal Delta Plain, India. *Applied Geochemistry* **61**: 87–98.

Gilliland K, Simpson IA, Adderley WP *et al.* 2013. The dry tank: development and disuse of water management infrastructure in the Anuradhapura hinterland, Sri Lanka. *Journal of Archaeological Science* **40**: 1012–1028.

Goldstein G, Santiago LS (eds). 2016. *Tropical Tree Physiology*. Springer: Cham.

GSMB. 1996. Colombo-Ratnapura 1:100,000 Geological Sheet (Provisional Series), Colombo, Geological Surveys and Mines Bureau, Sri Lanka.

He D, Ladd SN, Sachs JP. 2017. Inverse relationship between salinity and $^{2}H/^{1}H$ fractionation in leaf wax n-alkanes from Florida mangroves. *Organic Geochemistry* **110**: 1–12.

Jayatissa LP, Dahdouh-Guebas, Koedam N. 2002. A review of the floral composition and distribution of mangroves in Sri Lanka. *Botanical Journal of the Linnean Society* **138**: 29–43.

Johansen PG. 2010. Site maintenance practices and settlement social organization in Iron Age Karnataka, India: Inferring settlement places and landscape from surface distributions of ceramic assemblage attributes. *Journal of Anthropological Archaeology* **29**: 432–454.

Kumaran KPN, Nair KM, Shindikar M *et al.* 2005. Stratigraphical and palynological appraisal of the Late Quaternary mangrove deposits of the west coast of India. *Quaternary Research* **64**: 418–431.

Lucero LJ, Fletcher R, Coningham R. 2015. From 'collapse' to urban diaspora: the transformation of low-density, dispersed agrarian urbanism. *Antiquity* **89**: 1139–1154.

Malmgren BA, Hulugalla R, Hayashi Y *et al.* 2003. Precipitation trends in Sri Lanka since the 1870s and relationships to El Niño-southern oscillation. *International Journal of Climatology* **23**: 1235–1252.

Meyers P, Ishiwatari R. 1993. Lacustrine organic geochemistry - an overview of indicators of organic matter sources and diagenesis in lake sediments. *Organic Geochemistry* **20**: 867–900.

Meyers PA. 2003. Application of organic geochemistry to paleolimnological reconstruction: a summary of examples from the Laurention Great Lakes. *Organic Geochemistry* **34**: 261–289.

Mirza MMQ. 2011. Climate change, flooding in South Asia and implications. *Regional Environmental Change* **11**: 95–107.

Mishra PK, Ankit Y, Gautam PK *et al.* 2019. Inverse relationship between south-west and north-east monsoon during the late Holocene: Geochemical and sedimentological record from Ennamangalam Lake, southern India. *Catena* **182** 104117.

Moore PD, Webb JA, Collison ME. 1991. *Pollen analysis*. Blackwell Publishing: Oxford.

Moy CM, Seltzer GO, Rodbell DT *et al.* 2002. Variability of El Niño /Southern Oscillation activity at millennial timescales during the Holocene epoch. *Nature* **420**: 162–165.

Nguyen HT, Meir P, Sack L *et al.* 2017. Leaf water storage increases with salinity and aridity in the mangrove Avicennia marina: integration of leaf structure, osmotic adjustment and access to multiple water sources. *Plant Cell and Environment* **40**: 1576–1591.

Parida AK, Jha B. 2010. Salt tolerance mechanisms in mangroves: A review. *Trees - Structure and Function* **24**: 199–217.

Ponton C, Giosan L, Eglinton TI *et al.* 2012. Holocene aridification of India. *Geophysical Research Letters* **39**: 1–6.

Poynter J, Eglinton G. 1990. Molecular composition of three sediments from hole 717c: The Bengal fan. *Proceedings of the Ocean Drilling* 116: 155–161.

Prasad S, Anoop A, Riedel N *et al.* 2014. Prolonged monsoon droughts and links to Indo-Pacific warm pool: A Holocene record from Lonar Lake, central India. *Earth and Planetary Science Letters* **391**: 171–182.

Premathilake R, Gunatilaka A. 2013. Chronological framework of Asian Southwest Monsoon events and variations over the past 24,000 years in Sri Lanka and regional correlations. *Journal of the National Science Foundation of Sri Lanka* **41**: 219.

Premathilake R, Risberg J. 2003. Late Quaternary climate history of the Horton Plains, central Sri Lanka. *Quaternary Science Reviews* **22**: 1525–1541.

Ranasinghe PN, Ortiz JD, Moore AL *et al.* 2013. Mid–Late Holocene coastal environmental changes in southeastern Sri Lanka: New evidence for sea level variations in southern Bay of Bengal. *Quaternary International* **298**: 20–36.

Ranawana KB. 2017. Mangroves of Sri Lanka. *Publication of Seacology-Sudeesa Mangrove. Museum* **1**: 25–28.

Ranjan RK, Routh J, Val Klump J *et al.* 2015. Sediment biomarker profiles trace organic matter input in the Pichavaram mangrove complex, southeastern India. *Marine Chemistry* **171**: 44–57.

Ranwella SP. 1995. *A checklist of Vertebrates of Bolgoda South Lake Area*. Young Zoologists Association of Sri Lanka: Dehiwala.

Ratnayake U, Herath S. 2005. Changing rainfall and its impact on landslides in Sri Lanka. *Journal of Mountain Science* **2**: 218–224.

Ratnayake AS, Sampei Y, Ratnayake NP *et al.* 2017. Middle to late Holocene environmental changes in the depositional system of the tropical brackish Bolgoda Lake, coastal southwest Sri Lanka. *Palaeogeography, Palaeoclimatology, Palaeoecology* **465**: 122–137.

Ratnayake AS, Ratnayake NP, Sampei Y *et al.* 2018. Seasonal and tidal influence for water quality changes in coastal Bolgoda Lake system, Sri Lanka. *Journal of Coastal Conservation* **22**: 1191–1199.

Ratnayake AS, Sampei Y, Ratnayake NP. 2019. Characteristics of sedimentary organic matter and vascular plants in tropical brackish Bolgoda Lake, Sri Lanka: Implications for paleoecology and chemotaxonomy. *Regional Studies in Marine Science* **30** 100726.

Reimer PJ, Bard E, Bayliss A *et al.* 2013. IntCal13 and Marine13 radiocarbon age calibration curves 0–50,000 Years cal BP. *Radiocarbon* **55**: 1869–1887.

Roberts P. 2019. *Tropical forests in prehistory, history, and modernity*. Oxford University Press: Oxford.

Roberts P, Perera N, Wedage O *et al.* 2015. Direct evidence for human reliance on rainforest resources in late Pleistocene Sri Lanka. *Science* **347**: 1246–1249.

Setyaningsih CA, Biagioni S, Saad A *et al.* 2019. Response of mangroves to Late Holocene sea-level change: palaeoecological evidence from Sumatra, Indonesia. Wetlands.

Shaw R, Nguyen H (eds). 2011. Droughts in Asian monsoon region. Emerald Group Publishing.

Silva Jde, Sonnadara DUJ. 2016. Century scale climate change in the central highlands of Sri Lanka. *Journal of Earth System Science* **125**: 75–84.

Tierney JE, Russell JM, Huang Y *et al.* 2008. Northern Hemisphere controls on tropical southeast African climate during the past 60,000 years. *Science* **322**: 252–255.

Veena M, Achyuthan H, Eastoe C *et al.* 2014. A multi-proxy reconstruction of monsoon variability in the late Holocene, South India. *Quaternary International* **325**: 63–73.

Versteegh GJM, Schefuß E, Dupont L *et al.* 2004. Taraxerol and Rhizophora pollen as proxies for tracking past mangrove ecosystems. *Geochimica et Cosmochimica Acta* **68**: 411–422.

Wakeham SG, Peterson ML, Hedges JI *et al.* 2002. Lipid biomarker fluxes in the Arabian Sea, with a comparison to the equatorial Pacific Ocean. *Deep-Sea Research Part II: Topical Studies in Oceanography* **49**: 2265–2301.

Werner RA, Brand WA. 2001. Referencing strategies and techniques in stable isotope ratio analysis. *Rapid Communications in Mass Spectrometry* **15**: 501–519.

Zubair L, Ralapanawe V, Tennakoon U *et al.* 2006. Natural disaster risks in Sri Lanka: Mapping hazards and risk hotspots. *Natural Disaster Hotspots Case Studies* **109**.

 